


## Evidence for melting mud in Earth's mantle from extreme oxygen isotope signatures in zircon.

Item type	Article
Authors	Spencer, Christopher J.; Cavosie, Aaron J.; Raub, Timothy D.; Rollinson, Hugh; Jeon, Heejin; Searle, Michael P.; Miller, Jodie A.; McDonald, Bradley J.; Evans, Noreen J.
Citation	C.J. Spencer, A.J. Cavosie, T.D. Raub, H. Rollinson, H. Jeon, M.P. Searle, J.A. Miller, B.J. McDonald, N.J. Evans, ; Evidence for melting mud in Earth's mantle from extreme oxygen isotope signatures in zircon. <i>Geology</i> ; 45 (11): 975–978. doi:10.1130/G39402.1
DOI	<a href="https://doi.org/10.1130/G39402.1">10.1130/G39402.1</a>
Publisher	Geological Society of America
Journal	<i>Geology</i>
Downloaded	13-Jan-2019 02:44:04
Link to item	<a href="http://hdl.handle.net/10545/621958">http://hdl.handle.net/10545/621958</a>

Publisher: GSA  
Journal: GEOL: Geology  
DOI:10.1130/G39402.1

# Evidence for melting mud in Earth's mantle from extreme oxygen isotope signatures in zircon

C.J. Spencer<sup>1\*</sup>, A.J. Cavosie<sup>1,2</sup>, T.D. Raub<sup>3</sup>, H. Rollinson<sup>4</sup>, H. Jeon<sup>5</sup>, M.P. Searle<sup>6</sup>,  
J.A. Miller<sup>7</sup>, ~~B.J. McDonald<sup>89</sup>~~, and N.J. Evans<sup>89</sup> 

*The Institute of Geoscience Research (TIGeR), Department of Applied Geology, Curtin University, Perth, WA 6845, Australia*

*<sup>2</sup>NASA Astrobiology Institute, Department of Geoscience, University of Wisconsin-Madison, Madison, Wisconsin 53706, USA*

*<sup>3</sup>Department of Earth and Environmental Sciences, University of St Andrews, St Andrews KY16 9AL, UK*

*<sup>4</sup>Geoscience, University of Derby, Derby DE22 1GB, UK*

*<sup>5</sup>Centre for Microscopy, Characterisation and Analysis, University of Western Australia, Perth, WA 6009, Australia*

*<sup>6</sup>Department of Earth Sciences, University of Oxford, South Parks Road, Oxford OX1 3AN, UK*

*<sup>7</sup>Department of Earth Sciences, Stellenbosch University, Matieland, 7602 Stellenbosch, South Africa*

*<sup>8</sup>Edinburgh Ion Microprobe Facility, University of Edinburgh, Edinburgh EH9 3FE, UK*

*<sup>89</sup>GeoHistory Facility, John de Laeter Centre, Department of Applied Geology, Curtin University, Perth, WA 6102, Australia*

*<sup>9</sup>Edinburgh Ion Microprobe Facility, University of Edinburgh, Edinburgh EH9 3FE, UK*

## ABSTRACT

Melting of subducted sediment remains controversial, as direct observation of sediment melt generation at mantle depths is not possible. Geochemical fingerprints provide indirect evidence for subduction-delivery of sediment to the mantle, however sediment abundance in mantle-derived melt is generally low (0%–2%), and difficult to detect. Here we provide evidence for melting of subducted sediment in granite sampled from an exhumed mantle section. Peraluminous granite dikes that intrude peridotite in the Oman-United Arab Emirates ophiolite have U-Pb ages of  $99.8 \pm 3.3$  Ma that predate obduction. The dikes have unusually high oxygen isotope ( $\delta^{18}\text{O}$ ) values for whole rock (14–23‰) and quartz (20–22‰), and yield the highest  $\delta^{18}\text{O}$  zircon values known (14–28‰; values relative to VSMOW). The extremely high oxygen isotope ratios uniquely identify the melt source as high  $\delta^{18}\text{O}$  marine sediment (pelitic and/or siliceous mud), as no other source could produce granite with such anomalously high  $\delta^{18}\text{O}$ . Formation of high  $\delta^{18}\text{O}$  sediment-derived (S-type) granite within peridotite requires subduction of sediment to the mantle, where it melted and intruded overlying mantle wedge. The granite suite described here contains the highest oxygen isotope ratios reported for igneous rocks, yet intruded mantle peridotite below the Mohorovičić seismic discontinuity, the most primitive oxygen isotope reservoir in the silicate Earth. Identifying the presence and quantifying the extent of sediment melting within the mantle has important implications for understanding subduction recycling of supracrustal material and effects of on mantle heterogeneity over time.

## INTRODUCTION

Subduction of lithosphere to the upper mantle is a fundamental tenet of plate tectonics (Wilson, 1963). Detection of sediment contributions to mantle-derived melt

provides evidence for transport of sediment to the mantle via subduction. Geochemical tracers used to detect the presence of sediment in mantle melt (i.e., basalt) include trace elements (Ba, La, Th, and others, e.g., Plank and Langmuir, 1993), and isotopes ( $\delta^{18}\text{O}$ ,  $\delta^{37}\text{Cl}$ ,  $^{10}\text{Be}$ , and others, e.g., Eiler et al., 1995; John et al., 2010; Dreyer et al., 2010). Calculated sediment abundances in basalt are typically low, <2% (e.g., Eiler et al., 1995). Here, field observations, petrologic data, and oxygen isotope evidence are used to show that peraluminous granite dikes intruding peridotite in the Oman-United Arab Emirates (UAE) ophiolite formed by melting of subducted marine sediment in the mantle.

Opportunities to observe in situ melt generated in the mantle are rare, and generally restricted to ophiolites, sections of oceanic crust and mantle exposed at convergent plate margins (Dewey, 1976). The Oman-UAE ophiolite is considered the type-example of an ophiolite, consisting of a section of oceanic crust and mantle that was obducted onto the Arabian continental margin in the Late Cretaceous (Fig. 1A; Searle et al., 2015). The crustal section includes ~8 km of pillow basalt, sheeted dikes, and gabbro above the crust-mantle transition, or petrologic Moho. The underlying mantle section consists of ~15 km of peridotite (harzburgite), and hosts the dike suite studied here (Fig. 1B).

Three distinct suites of granites (*sensu latu*) are recognized in the Oman-UAE ophiolite. Granites intruding the crustal section form a ‘crustal plagiogranite’ suite that ranges from granodiorite to tonalite, has  $\text{SiO}_2$  from 54 to 72 wt.%, and low  $\text{K}_2\text{O}$  (<1 wt.%). The crustal plagiogranite suite is metaluminous, contains zircon with  $\delta^{18}\text{O}$  from ~4–5‰, and formed by fractionation of mantle melt or anatexis of oceanic crust (Grimes et al., 2013; Rollinson, 2015). Two additional suites intrude peridotite; one has  $\text{SiO}_2$  from



67%–75%, is metaluminous, and ranges from granodiorite to tonalite. The other suite intrusive to the mantle and the focus of this study has higher SiO<sub>2</sub> values (72%–78%), it is peraluminous and is predominately true granite (*sensu stricto*), consisting of near-equal proportions of quartz, plagioclase, and alkali feldspar (Cox et al., 1999; Rollinson, 2015; Searle et al., 2015). The origin of the peraluminous suite is debated; proposed formation mechanisms include fractionation from mafic melt (Peters and Kamber, 1994), anatexis of pelitic material (Cox et al., 1999; Searle et al., 2015), and mixtures of melted crust and sediment (Rollinson, 2015; Haase et al., 2015). A key observation recognized from field studies (Peters and Kamber, 1994) and confirmed by zircon U/Pb dating (Styles et al., 2006; Rioux et al., 2013; this study) is that granite in the mantle section formed synchronous with ocean crust formation at ca. 99 Ma, and thus pre-date ophiolite obduction from ca. 85–90 Ma (Searle et al., 2015; Styles et al., 2006). The pre-obduction intrusive relationship distinguishes the Oman-UAE granite suite from other ophiolites where granite intruded peridotite post-obduction (e.g., Ronda peridotite, Priem et al., 1979).

## METHODS AND SAMPLES

We present  $\delta^{18}\text{O}$ , U-Pb, trace element, and  $\epsilon\text{Hf}$  data for zircon, and  $\delta^{18}\text{O}$  for whole rock and quartz from ten dike samples (see the GSA data repository<sup>1</sup> item DR1 for methods). Zircon grains were imaged by scanning electron microscopy, analyzed for oxygen isotope ratio using secondary ion mass spectrometry (SIMS), and U-Pb age, trace element, and  $\epsilon\text{Hf}$  by laser ablation inductively couple plasma mass spectrometry (LA-

ICPMS) (Items DR1, DR2). Analyses of whole rock and quartz for oxygen isotope ratio were made by laser fluorination (Items DR1, DR2).

Ten peraluminous granite dikes along a ~250 km length of the mantle section of the Oman-UAE ophiolite were analyzed (Fig. 1; Item DR1). The dikes range from 2 to 8 m in width (Fig. 1B). Major and trace element data for dikes at each of the three sampling sites (our samples with prefixes 13- and 14-) were reported previously (Rollinson, 2015).

The granite dikes are uniformly peraluminous ( $\text{Al}_2\text{O}_3/\text{Na}_2\text{O}+\text{K}_2\text{O}+\text{CaO} > 0.99$ ), high in  $\text{SiO}_2$  (~74%–77% wt.%), **generally** low in Fe, Mg, Ca, and Na, and all but one has normative corundum (0.4%–0.9%) (Item DR1). The peraluminous granites contain accessory minerals such as muscovite, biotite, garnet, cordierite, andalusite, lepidolite, tourmaline, and zircon (Rollinson, 2015; Item DR1). Some samples exhibit evidence of alteration of various minerals to secondary phases.

## RESULTS

### **Zircon U-Pb, trace elements, and $\epsilon\text{Hf}$ by LA-ICPMS**

Zircon grains from **seven five** samples were analyzed for U/Pb, targeting both cores and rims and yield a  $^{206}\text{Pb}/^{238}\text{U}$  age of  $99.8 \pm 3.3$  Ma ( $2\sigma$ , MSWD = 1.7;  $n = 16$ ; Fig. 1C). The same grains yield **rare earth element and Ti abundances typical for crustal zircon and**  $\epsilon\text{Hf}$  values **range**ing from 2.8 to –4.4 ( $n = 16$ ; Item DR1). No evidence of inheritance was detected within analytical uncertainty.

**Zircon  $\delta^{18}\text{O}$  by SIMS** for individual 15  $\mu\text{m}$  spots on zircon grains ranges from  $13.8 \pm 0.5\text{‰}$  to  $27.0 \pm 0.7\text{‰}$  ( $2\sigma$ ), with a mean zircon  $\delta^{18}\text{O}$  for the suite of  $19.7 \pm 2.9\text{‰}$  ( $1\sigma$ ,  $n = 125$  analyses on 112 zircon grains; Figure 2; Items DR1, 2). Grains in most samples

record minor within-sample variation of  $\delta^{18}\text{O}$  ( $<2\%$ ), whereas in some samples grain-to-grain variability is up to 11%. Variable  $\delta^{18}\text{O}$  values also occur within individual grains (Fig. 3A). Multi-spot analysis shows that some grains are homogenous in  $\delta^{18}\text{O}$ , whereas others are zoned by up to  $\sim 9\%$  (item DR1). The highest  $\delta^{18}\text{O}$  zircon (Fig. 3A) was analyzed an additional 57 times using a  $\sim 3\text{ }\mu\text{m}$  spot (Fig. 3B), with  $\delta^{18}\text{O}$  ranging from  $17.7 \pm 1.6\%$  to  $30.7 \pm 1.5\%$  in a concentric pattern. The  $\sim 3\text{ }\mu\text{m}$  spot analyses reveal a 28‰ core surrounded by a 19‰ rim (Fig. 3C). Concurrent analysis of  $^{16}\text{O}^1\text{H}/^{16}\text{O}$  yielded low background-corrected values (0–0.0006), which showed no significant deviation during the 57 analyses, indicating the core is not metamict ([Wang et al., 2014](#); see Item DR1).

#### **Whole Rock and Quartz $\delta^{18}\text{O}$ by Laser Fluorination**

Measured whole rock granite and quartz  $\delta^{18}\text{O}$  values range from 14.3 to 19.3‰ and 19.9–22.1‰, respectively (Fig. 2B). The whole rock  $\delta^{18}\text{O}$  values are uniformly high for igneous rocks, although some are lower than predicted based on zircon; the range of measured zircon  $\delta^{18}\text{O}$  values for high-silica granites ( $\sim 76\text{ wt.}\%$   $\text{SiO}_2$ ) would be in equilibrium with whole rock  $\delta^{18}\text{O}$  ranging from 16 to 29‰ (Valley et al., 2005). Some of the whole rock and quartz  $\delta^{18}\text{O}$  values thus record high temperature equilibrium with zircon, whereas others reflect variable exchange during sub-solidus alteration.

## **DISCUSSION**

### **High $\delta^{18}\text{O}$ S-type Granite in the Oman UAE Ophiolite**

The Oman-UAE peraluminous granite dike suite described here (Fig. 2B) are the highest  $\delta^{18}\text{O}$  igneous rocks known (Cavosie et al., 2011). The previously reported highest

$\delta^{18}\text{O}$  values for igneous zircon (~14‰), quartz (~18‰), and whole rock (~16‰) are from ~1.2 billion year old granitoids of the Frontenac terrane in Ontario, Canada (Fig. 2B; Peck et al., 2004). Formation of the high  $\delta^{18}\text{O}$  Frontenac granitoids is attributed to subduction and melting of continental material during accretionary orogeny. Mean values presented here for zircon (~20‰), quartz (~21‰), and whole rock (~17‰) are significantly higher than those found in Frontenac granitoids.

All available geochemical data for the granite dikes, including high  $\delta^{18}\text{O}$ , peraluminous character, normative corundum, the presence of aluminous minerals (garnet, muscovite and andalusite), and low Fe, Mg, Ca, and Na, identify the suite as S-type granite, having originated through melting of supracrustal materials (Chappell and White, 1974). Identification of crustal Nd and Hf isotope signatures (Haase et al., 2015) and elevated trace element abundance (Rollinson, 2015) in studies of peraluminous granite from the Oman-UAE ophiolite further support their classification as S-type granite.

Previous studies of zircon in S-type granite have found anomalously large intra-sample variation in igneous  $\delta^{18}\text{O}$  (up to 5‰), with ubiquitous inherited cores (e.g., Appleby et al., 2010). The S-type granites reported here show even greater intra-sample variation in zircon  $\delta^{18}\text{O}$ , from 14 to 28‰, including grains zoned by 9‰ (Fig. 3). The granites reported here are further distinguished from any other S-type granite in that the unimodal U-Pb ages preclude a detrital origin for the high  $\delta^{18}\text{O}$  zircon; no evidence of inheritance was detected.

## **Oxygen Isotopes Constrain a Sediment Source**

We hypothesize that high  $\delta^{18}\text{O}$  pelagic mud (pelitic and/or siliceous) was subducted and melted below rapidly forming ocean crust during slab rollback (Rioux et al., 2013; Searle et al., 2015). The high  $\delta^{18}\text{O}$  values measured for zircon, quartz, and whole rock uniquely restrict the melt source of the peraluminous granite suite to high  $\delta^{18}\text{O}$  sediment. The extremely elevated  $\delta^{18}\text{O}$  signatures for igneous zircon exclude a mantle source, as whole rock values for peridotite and derivative melts do not exceed  $\sim 6\text{‰}$  (Valley et al., 2005). A global survey of whole rock values identifies shale ( $\delta^{18}\text{O}$  up to  $26\text{‰}$ ; Payne et al., 2015) as the most likely high  $\delta^{18}\text{O}$  source that would yield peraluminous granite when melted (Nichols et al., 1994). Other possible high  $\delta^{18}\text{O}$  sources include siliceous and carbonate oozes, which have whole rock  $\delta^{18}\text{O}$  values from 25 to  $42\text{‰}$  (Eiler, 2000). However, melts of oozes or lithified equivalents would not form peraluminous granite, which limits their contributions, if present. Linear mixing of equal parts altered basalt (50 wt%  $\text{SiO}_2$ ,  $\delta^{18}\text{O} = \sim 9\text{‰}$ ) and chert (100 wt%  $\text{SiO}_2$ ,  $\delta^{18}\text{O} = \sim 40\text{‰}$ ) could produce a  $\delta^{18}\text{O}$  melt ( $\sim 21\text{‰}$ ) in equilibrium with the mean zircon  $\delta^{18}\text{O}$  ( $\sim 19\text{‰}$ , Fig. 2), however  $\text{SiO}_2$  would be too low (70 wt. %), and equilibrium with the highest zircon  $\delta^{18}\text{O}$  value (Fig. 3) is not attainable. More reasonable melt components include shale (60 wt%  $\text{SiO}_2$ ,  $\delta^{18}\text{O} = \sim 20\text{‰}$ ) mixed with 30%–40% chert, which could produce a melt with  $\sim 75$  wt%  $\text{SiO}_2$  and whole rock  $\delta^{18}\text{O}$  of up to  $\sim 28\text{‰}$ . Regardless of lithologies chosen for modeling or extent of melting (partial versus bulk), unusually high  $\delta^{18}\text{O}$  sources are required to crystallize the  $\sim 28$  to  $19\text{‰}$  zircon domains. The zircon core-~~to~~-rim

relationships indicate the source was clearly heterogeneous, resulting in melt  $\delta^{18}\text{O}$  changing evolved over time, either in the dynamic environment of the subduction channel or in the overlying mantle wedge.

No appreciable volume of shale is exposed near the Oman-UAE ophiolite on the paleo-continental shelf (Searle et al., 2015; Searle and Cox, 1999). Siliceous schist, marble, and chert, all with high whole rock  $\delta^{18}\text{O}$ , occur regionally (Grantham et al. 2003), however these lithologies do not have an appropriate composition to form S-type granite when melted (Rollinson, 2015). The lack of shale in the region is not surprising, as the majority of pelagic pelitic mud in modern marine settings is found further offshore and would have been among the first continentally-derived material subducted at ~99 Ma. Pelagic zircon-free sediment from the Arabian continent is consistent with  $\epsilon_{\text{Hf}}$  values and lack of age inheritance (Fig. 1C; Item DR1).

### **Melting Mud in the Mantle**

Data presented here from the Oman-UAE ophiolite provide direct geochemical evidence for melting of subducted sediment within the mantle from an intact section of mantle lithosphere. Prior estimates for sediment components in the Oman-UAE mantle granite suites range from 10%–30% (trace elements, Rollinson, 2015), to near 80% (Hf-Nd isotopes, Haase et al., 2015), however our results constitute the first report of pure sediment melting. Oxygen isotopes are a highly sensitive tracer of melt source; no indication of mantle-derived melt was detected in the peraluminous granite suite, nor is one required, as the granite compositions can be fully explained by melting of high  $\delta^{18}\text{O}$  marine sediment. The peraluminous granite suite described here may thus represent the

first report of S-type granite that contains no detectable component of ‘primitive melt’  
(c.f. Kemp et al., 2008).

Recognition of the peraluminous granite dikes as nearly pure sediment melts may lead to new insights into related subduction zone processes, including constraining the steady-state volume of subducted sediment needed to source the melts, and the rheology and thermal state of the mantle wedge to allow for semi-brittle fracture formation and propagation during dike emplacement. The initiation of subduction, formation of oceanic crust, melting of sedimentary material, and intrusion of S-type granite into the mantle wedge all pre-date thrusting of the oceanic crust onto the Arabian continental margin to form the Oman-UAE ophiolite (Searle et al., 2015; Searle and Cox, 1999). These data thus provide “ground truth” confirmation for sediment subduction and melting beneath supra-subduction zone ophiolites (Furnes and Dilek, 2017). The recognition that small-volume, isotopically evolved, granitoid reservoirs form in the upper mantle as a consequence of subduction also has implications for the compositional heterogeneity of the mantle over time.

## ACKNOWLEDGMENTS

The British Geological Survey, in particular Bob B. Thomas, is thanked for providing materials. We thank Tanya T. Claridge, Rich R. Taylor, Chris C. Harris, Torsten T. Vennemann, Benita B. Pulitz, Carl C. Hoiland, and Tyler T. Ambrose for assistance, access to facilities, and helpful conversations. Camille Spencer assisted with fieldwork. GeoHistory Facility instruments were funded via an AGOS grant provided to AuScope by the AQ44 Australian EIF. AMMRF, AuScope, SIEF, and the State Government of Western Australia contributed funding to CMCA at UWA. Funding is

acknowledged from the NERC EIMF (IMF 544–1114) to TR and the Fondation Herbette  
to JM. We thank J. Hermann, O. Jagoutz, an ~~and an~~ anonymous review, and editor J.  
Totman Parrish for excellent comments.

## REFERENCES CITED

- Appleby, S.K., Gillespie, M.R., Graham, C.M., Hinton, R.W., Oliver, G.J.H., Kelly,  
N.M., and EIMF, 2010, Do S-type granites commonly sample infracrustal sources?:  
New results from an integrated O, U-Pb and Hf isotope study of zircon:  
Contributions to Mineralogy and Petrology, v. 160, p. 115–132, doi:10.1007/s00410-  
009-0469-3.
- Cavosie, A.J., Valley, J.W., Kita, N.T., Spicuzza, M.J., Ushikubo, T., and Wilde, S.A.,  
2011, The origin of high  $\delta^{18}\text{O}$  zircons: Marbles, megacrysts, and metamorphism:  
Contributions to Mineralogy and Petrology, v. 162, p. 961–974, doi:10.1007/s00410-  
011-0634-3.
- Chappell, B., and White, A., 1974, Two contrasting granite types: Pacific Geology, v. 8,  
p. 173–174.
- Cox, J., Searle, M., and Pedersen, R., 1999, The petrogenesis of leucogranitic dykes  
intruding the northern Semail ophiolite, United Arab Emirates: field relationships,  
geochemistry and Sr/Nd isotope systematics: Contributions to Mineralogy and  
Petrology, v. 137, p. 267–287, doi:10.1007/s004100050550.
- Dewey, J.F., 1976, Ophiolite obduction: Tectonophysics, v. 31, p. 93–120,  
doi:10.1016/0040-1951(76)90169-4.
- Dreyer, B.M., Morris, J.D., and Gill, J.B., 2010, Incorporation of subducted slab-derived  
sediment and fluid in arc magmas: B–Be– $^{10}\text{Be}$ – $\epsilon\text{Nd}$  systematics of the Kurile



convergent margin, Russia: *Journal of Petrology*, v. 51, p. 1761–1782,

doi:10.1093/petrology/egq038.

Eiler, J.M., Farley, K.A., Valley, J.W., Stolper, E.M., Hauri, E.H., and Craig, H., 1995,

Oxygen isotope evidence against bulk recycled sediment in the mantle sources of

Pitcairn Island lavas: *Nature*, v. 377, p. 138–141, doi:10.1038/377138a0.

Eiler, J., 2001, Oxygen isotope variations of basaltic lavas and upper mantle rocks, in  
Reviews in Mineralogy and geochemistry, 43.1: 319-364.

Furnes, H., and Dilek, Y., 2017, Geochemical characterization and petrogenesis of

intermediate to silicic rocks in ophiolites: A global synthesis: *Earth-Science*

*Reviews*, v. 166, p. 1–37, doi:10.1016/j.earscirev.2017.01.001.

Grantham, G.H., Goedhart, M.L., Wipplinger, R.J., Thomas, R.J., Eglington, B.M.,

Harmer, R.E., and Hartzer, F.J., 2003, *The Surface Geology of the Emirate of*

*Fujairah*. Unpublished Report: Department of Industry and Economy, Government of

*Fujairah*, United Arab Emirates, 455 p.

Grimes, C.B., Ushikubo, T., Kozdon, R., and Valley, J.W., 2013, Perspectives on the

origin of plagiogranite in ophiolites from oxygen isotopes in zircon: *Lithos*, v. 179,

p. 48–66, doi:10.1016/j.lithos.2013.07.026.

Haase, K.M., Freund, S., Koepke, J., Hauff, F., and Erdmann, M., 2015, Melts of

sediments in the mantle wedge of the Oman ophiolite: *Geology*, v. 43, p. 275–278,

doi:10.1130/G36451.1.

John, T., Layne, G.D., Haase, K.M., and Barnes, J.D., 2010, Chlorine isotope evidence

for crustal recycling into the Earth's mantle: *Earth and Planetary Science Letters*,

v. 298, p. 175–182, doi:10.1016/j.epsl.2010.07.039.

Kemp, A.I.S., Hawkesworth, C.J., Paterson, B.A., Foster, G.L., Kinny, P.D., Whitehouse, M.J., and Maas, R., 2008, Exploring the plutonic–volcanic link: A zircon U–Pb, Lu–Hf and O isotope study of paired volcanic and granitic units from southeastern Australia: Transactions of the Royal Society of Edinburgh. Earth Sciences, v. 97, p. 337–355, doi:10.1017/S0263593300001498.

Nichols, G.T., Wyllie, P.J., and Stern, C.R., 1994, Subduction zone melting of pelagic sediments constrained by melting experiments: Nature, v. 371, p. 785–788, doi:10.1038/371785a0.

Payne, J.L., Hand, M., Pearson, N.J., Barovich, K.M., and McInerney, D.J., 2015, Crustal thickening and clay: Controls on O isotope variation in global magmatism and siliciclastic sedimentary rocks: Earth and Planetary Science Letters, v. 412, p. 70–76, doi:10.1016/j.epsl.2014.12.037.

Peck, W.H., Valley, J.W., Corriveau, L., Davidson, A., McLelland, J., and Farber, D.A., 2004, Oxygen-isotope constraints on terrane boundaries and origin of 1.18–1.13 Ga granitoids in the southern Grenville Province: Geological Society of America, v. 197, p. 163–182.

Peters, T., and Kamber, B.S., 1994, Peraluminous potassium-rich granitoids in the Semail Ophiolite: Contributions to Mineralogy and Petrology, v. 118, p. 229–238, doi:10.1007/BF00306644.

- 295 Plank, T., and Langmuir, C.H., 1993, Tracing trace elements from sediment input to  
296 volcanic output at subduction zones: *Nature*, v. 362, p. 739–743,  
297 doi:10.1038/362739a0.
- 298 Priem, H.N.A., Boelrijk, N., Hebeda, E.H., Oen, I.S., Verdurmen, E.A.T., and Verschure,  
299 R.H., 1979, Isotopic dating of the emplacement of the ultramafic masses in the  
300 Serrania de Ronda, southern Spain: *Contributions to Mineralogy and Petrology*,  
301 v. 70, p. 103–109, doi:10.1007/BF00371876.
- 302 Rioux, M., Bowring, S., Kelemen, P., Gordon, S., Miller, R., and Dudás, F., 2013,  
303 Tectonic development of the Samail ophiolite: High-precision U-Pb zircon  
304 geochronology and Sm-Nd isotopic constraints on crustal growth and emplacement:  
305 *Journal of Geophysical Research. Solid Earth*, v. 118, p. 2085–2101,  
306 doi:10.1002/jgrb.50139.
- 307 Rollinson, H., 2015, Slab and sediment melting during subduction initiation: Granitoid  
308 dykes from the mantle section of the Oman ophiolite: *Contributions to Mineralogy*  
309 *and Petrology*, v. 170, p. 32–52, doi:10.1007/s00410-015-1177-9.
- 310 Searle, M.P., Waters, D.J., Garber, J.M., Rioux, M., Cherry, A.G., and Ambrose, T.K.,  
311 2015, Structure and metamorphism beneath the obducting Oman ophiolite: Evidence  
312 from the Bani Hamid granulites, northern Oman mountains: *Geosphere*, v. 11,  
313 p. 1812, doi:10.1130/GES01199.1.
- 314 Searle, M., and Cox, J., 1999, Tectonic setting, origin, and obduction of the Oman  
315 ophiolite: *Geological Society of America Bulletin*, v. 111, p. 0104–0122,  
316 doi:10.1130/0016-7606(1999)111<0104:TSOAOO>2.3.CO;2.

Spencer, C.J., Cawood, P.A., Hawkesworth, C.J., Raub, T.D., Prave, A.R., and Roberts,  
N.M.W., 2014, Proterozoic onset of crustal reworking and collisional tectonics:  
Reappraisal of the zircon oxygen isotope record: *Geology*, v. 42, p. 451–454,  
doi:10.1130/G35363.1.

Styles, M., Ellison, R., Arkley, S., Crowley, Q.G., Farrant, A., Goodenough, K.M.,  
McKervey, J., Pharaoh, T., Phillips, E., and Schofield, D., 2006, The geology and  
geophysics of the United Arab Emirates: Volume 2, *geology*: v. 7, no. November.

Valley, J.W., Lackey, J.S., Cavosie, A.J., Clechenko, C.C., Spicuzza, M.J., Basei,  
M.A.S., Bindeman, I.N., Ferreira, V.P., Sial, A.N., King, E.M., Peck, W.H., Sinha,  
A.K., and Wei, C.S., 2005, 4.4 billion years of crustal maturation: Oxygen isotope  
ratios of magmatic zircon: *Contributions to Mineralogy and Petrology*, v. 150,  
p. 561–580, doi:10.1007/s00410-005-0025-8.

Wilson, J.T., 1963, Hypothesis of Earth's Behaviour: *Nature*, v. 198, p. 925–929,  
doi:10.1038/198925a0.

FIGURE CAPTIONS

Figure 1. A: Simplified map of the Oman-UAE ophiolite (Rollinson, 2015) with locations of sampling sites. B: Photograph of peraluminous granite intruding mantle peridotite (harzburgite) near Al-Dadnah, UAE. C: Terra-Wasserberg concordia of U-Pb data for granite samples from this study.

Figure 2. A: Histogram of  $\delta^{18}\text{O}$  zircon analyses (15  $\mu\text{m}$  SIMS spots) from peraluminous granite in this study compared with global  $\delta^{18}\text{O}$  compilations of igneous (Cavosie et al., 2011) and detrital (Spencer et al., 2014) zircon data. Note that 99.8% of detrital and 100% of igneous grains are below 13.8‰, the lowest measured  $\delta^{18}\text{O}$  values of zircon from the peraluminous granite reported here. B: Zircon, quartz, and whole rock  $\delta^{18}\text{O}$  values from Frontenac terrane granitoids (Peck et al., 2004) and peraluminous granite (this study).

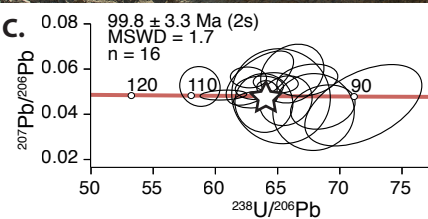
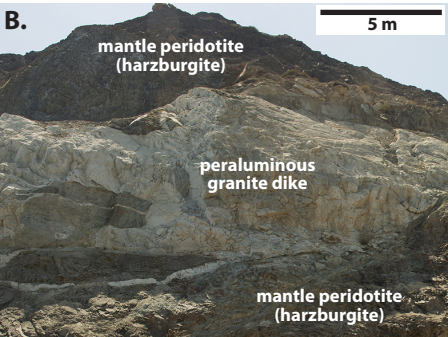
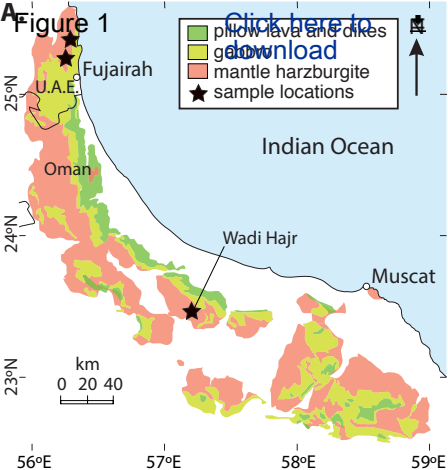
Figure 3. A: Cathodoluminescence (CL) image of zircon UAE436\_1, displaying locations of the three 15  $\mu\text{m}$   $\delta^{18}\text{O}$  spots. Faint growth zoning in the dark core parallels zoning in rim, indicating primary magmatic growth rather than inheritance. B: Backscatter electron image showing the fifty-seven  $\sim 3$   $\mu\text{m}$  spot analyses for  $\delta^{18}\text{O}$ . C: CL image of the same surface shown in B with color-coded analytical spots based upon the color scale. The spot with a cross in C is excluded, as it overlapped an inclusion visible in B. A histogram and kernel density estimation (dashed curve) are shown right of the color scale (bin- and bandwidth = 1.5‰). Background corrected  $^{16}\text{O}^1\text{H}/^{16}\text{O}$  (using  $\delta^{18}\text{O}$  standard 91500) is shown as a function of  $\delta^{18}\text{O}$  (vertical line) and is nearly invariant. All  $\delta^{18}\text{O}$  values are in ‰, with average uncertainties shown in A and B.

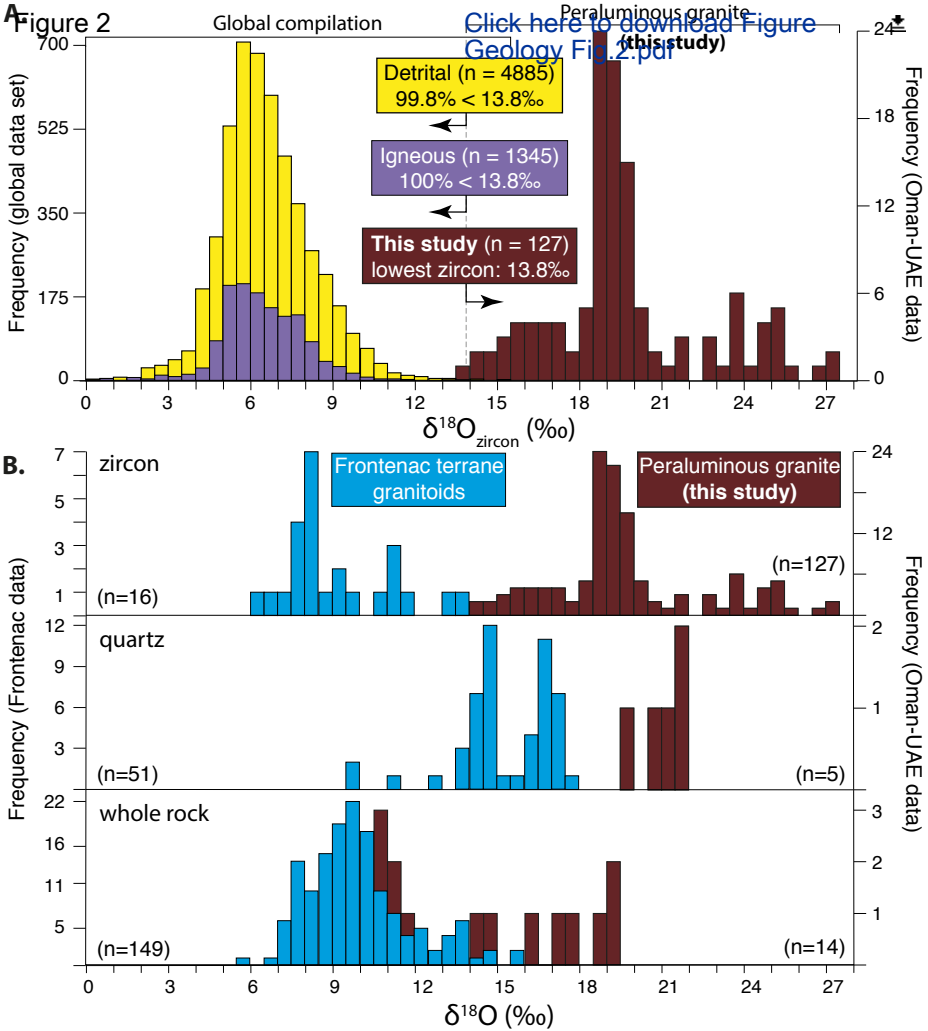
362

363 1GSA Data Repository item 2017xxx, material, methods, and full data tables, is available

364 online at <http://www.geosociety.org/datarepository/2017/> or on request from

365 [editing@geosociety.org](mailto:editing@geosociety.org).







**A** Figure 3

